

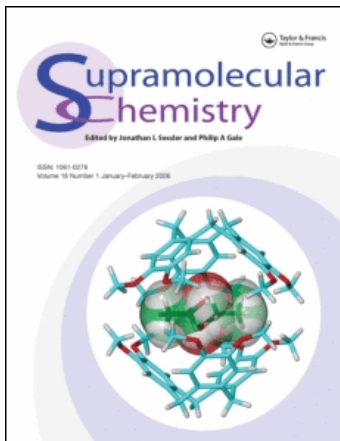
This article was downloaded by:

On: 29 January 2011

Access details: *Access Details: Free Access*

Publisher *Taylor & Francis*

Informa Ltd Registered in England and Wales Registered Number: 1072954 Registered office: Mortimer House, 37-41 Mortimer Street, London W1T 3JH, UK



## Supramolecular Chemistry

Publication details, including instructions for authors and subscription information:

<http://www.informaworld.com/smpp/title~content=t713649759>

### Diverse Modes of Guest Inclusion in a Cyclodextrin: X-ray Structural and Thermal Characterization of a 4:3 $\beta$ -cyclodextrin–Cyclizine Complex

Mino R. Caira<sup>a</sup>; Devric R. Dodds<sup>a</sup>; L. R. Nassimbeni<sup>a</sup>

<sup>a</sup> Department of Chemistry, University of Cape Town, Rondebosch, South Africa

**To cite this Article** Caira, Mino R. , Dodds, Devric R. and Nassimbeni, L. R.(2011) 'Diverse Modes of Guest Inclusion in a Cyclodextrin: X-ray Structural and Thermal Characterization of a 4:3  $\beta$ -cyclodextrin–Cyclizine Complex', *Supramolecular Chemistry*, 13: 1, 61 – 70

**To link to this Article:** DOI: 10.1080/10610270108034883

**URL:** <http://dx.doi.org/10.1080/10610270108034883>

PLEASE SCROLL DOWN FOR ARTICLE

Full terms and conditions of use: <http://www.informaworld.com/terms-and-conditions-of-access.pdf>

This article may be used for research, teaching and private study purposes. Any substantial or systematic reproduction, re-distribution, re-selling, loan or sub-licensing, systematic supply or distribution in any form to anyone is expressly forbidden.

The publisher does not give any warranty express or implied or make any representation that the contents will be complete or accurate or up to date. The accuracy of any instructions, formulae and drug doses should be independently verified with primary sources. The publisher shall not be liable for any loss, actions, claims, proceedings, demand or costs or damages whatsoever or howsoever caused arising directly or indirectly in connection with or arising out of the use of this material.

# Diverse Modes of Guest Inclusion in a Cyclodextrin: X-ray Structural and Thermal Characterization of a 4:3 $\beta$ -cyclodextrin – Cyclizine Complex

MINO R. CAIRA\*, DEVRIC R. DODDS and L. R. NASSIMBENI

*Department of Chemistry, University of Cape Town, Rondebosch 7701, South Africa*

1-Diphenylmethyl-4-methylpiperazine (cyclizine) is an antiemetic drug which forms an inclusion complex with  $\beta$ -cyclodextrin of formula  $(\beta\text{-cyclodextrin})_4 \cdot (\text{cyclizine})_3 \cdot 50\text{H}_2\text{O}$ . This species crystallizes in the monoclinic space group  $P2_1$  with  $a = 15.246(1)$ ,  $b = 65.075(5)$ ,  $c = 15.609(1)$  Å,  $\beta = 102.62(1)^\circ$  and  $Z = 2$  formula units. Complex water content and the host:drug stoichiometric ratio were determined by thermogravimetry and UV spectrophotometry respectively. Differential scanning calorimetry showed that the crystals dehydrate in at least two stages and begin to decompose from approximately 250°C. The crystal structure was solved by a combination of Patterson search and direct methods. Isotropic refinement converged at  $R = 0.094$  for 8806 reflections with  $I > 2\sigma(I)$ . The unusual stoichiometry is accounted for as follows: the four  $\beta$ -cyclodextrin molecules comprising the asymmetric unit occur as two independent head-to-head dimers, each formed by O–H...O hydrogen bonding across the macrocyclic secondary surfaces. One dimer contains two cyclizine guest molecules in head-to-tail orientation, thus accounting for two distinct modes of drug inclusion. In the second dimer, only one  $\beta$ -cyclodextrin molecule is significantly occupied by a cyclizine molecule (in a mode analogous to one of those in the first dimer), the other half of the dimer being largely devoid of guest. A possible mechanism for the formation of this unusual structure is proposed and

the crystal packing arrangement is shown to be based on a novel disrupted tetrameric channel motif.

*Keywords:*  $\beta$ -cyclodextrin; Cyclizine complex; Tetramer; X-ray structure; Thermal analysis

## INTRODUCTION

Inclusion of drug molecules in cyclodextrins (CDs) continues to be commercially exploited as a means of improving guest performance (solubility, bioavailability, chemical stability) [1]. Structural characterization to demonstrate the formation of a true inclusion complex is mandatory when the complex is intended for medicinal use [2], and under favorable conditions, X-ray diffraction can provide the necessary information unequivocally. We have used single crystal X-ray analysis to demonstrate CD-inclusion of drugs from various therapeutic classes *e.g.*, non-steroidal anti-inflammatories (diclofenac sodium [3], ibuprofen [4], naproxen [5]), antilipidemics

\*Corresponding author.

(clofibrilic acid [6]) and analgesics (*p*-bromoacetanilide [7], paracetamol [8]).

This report describes the preparation, and the thermal and X-ray structural characterization of an inclusion complex formed between the antiemetic drug cyclizine (1-diphenylmethyl-4-methylpiperazine, Fig. 1) and  $\beta$ -cyclodextrin. Since the aqueous solubility of cyclizine is very low ( $< 1 \text{ mg cm}^{-3}$  at  $25^\circ\text{C}$ ) and rapid onset of action is desirable for treating motion sickness, CD-inclusion is being explored as a possible strategy for improving the drug bioavailability [9].

The most common host-guest stoichiometry for  $\beta$ -CD complexes with known crystal structure is 1:1 [10]. This ratio is usually manifested in the crystal by the occurrence of either one specific host-guest motif repeated by space group symmetry (monomeric complexes) or by a pair of guest molecules (possibly with slightly different conformations and extents of inclusion) within a dimeric host 'basket' formed by head-to-head hydrogen bonded association (dimeric complexes) [10, 11]. It was therefore intriguing to discover that the title compound had a 4:3 host-guest ratio, since this suggested the possibility of multiple modes of guest inclusion. The results of the present study confirm this and also demonstrate that it is possible for a virtually 'empty'  $\beta$ -CD molecule to exist in a crystalline complex. The crystallographic results together with data from a modelling study of the inclusion of cyclizine in cyclodextrins [12] are used in an attempt to rationalize the formation of the asymmetric unit.

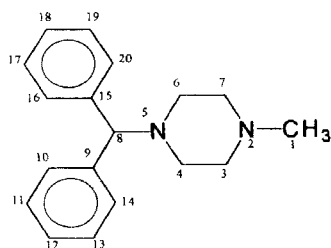


FIGURE 1 Structure of cyclizine and atomic numbering.

## RESULTS

### Thermal Analysis

The combined TG and DSC traces for the complex are shown in Figure 2. TG weight loss in the temperature range  $30\text{--}130^\circ\text{C}$  corresponds to crystal dehydration, as confirmed by preliminary thermomicroscopy. The DSC trace indicates that the water loss (peak A) is at least a two-step process since the endotherm has a shoulder at  $114^\circ\text{C}$  in addition to the main peak at  $82^\circ\text{C}$ . The anhydrous complex begins to decompose at  $250^\circ\text{C}$  (endotherm B), this event also being confirmed by thermomicroscopy which showed a distinct color change of the crystals from white to brown during heating. Further decomposition is accompanied by a shallow exotherm (C,  $270^\circ\text{C}$ ) and a series of endotherms (D,  $330^\circ\text{C}$  onwards).

### X-ray Analysis: Overall Description of Guest Inclusion Modes

Figures 3 and 4 are space filling diagrams showing occupation of the two crystallographically independent  $\beta$ -CD dimers by the three distinct guest molecules. Association of  $\beta$ -CD molecules into dimers by  $\text{O}\cdots\text{H}\cdots\text{O}$  hydrogen bonding across the secondary faces occurs frequently in  $\beta$ -CD inclusion complexes [11]. One of the dimers (Fig. 3) comprises  $\beta$ -CD molecules CD(A), CD(B) and contains a single cyclizine guest molecule, referred to as CYC(B). The second dimer (Fig. 4) consists of  $\beta$ -CD molecules CD(C), CD(D) which are included by guest molecules CYC(C) and CYC(D) respectively. In all cases, it is the methylpiperazine moiety of the guest which inserts into the  $\beta$ -CD cavity, leaving the diphenylmethyl residue protruding from the cavity.

In the CD(A)–CD(B) dimer, the major portion of the drug molecule is contained within the host molecule CD(B). The methyl group protrudes from the primary face of CD(B) while the

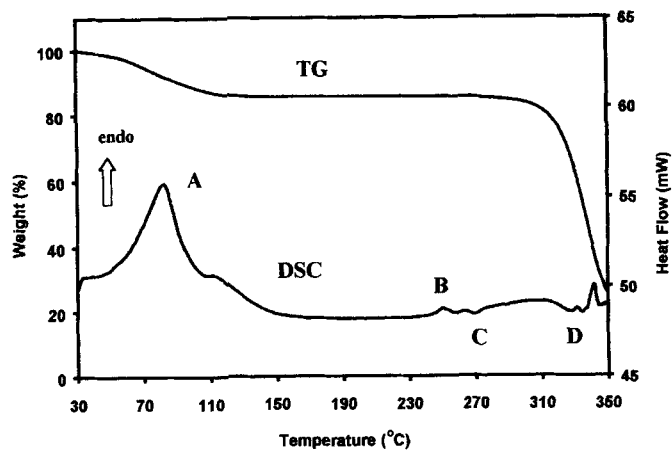


FIGURE 2 Combined TG/DSC trace for the title complex.

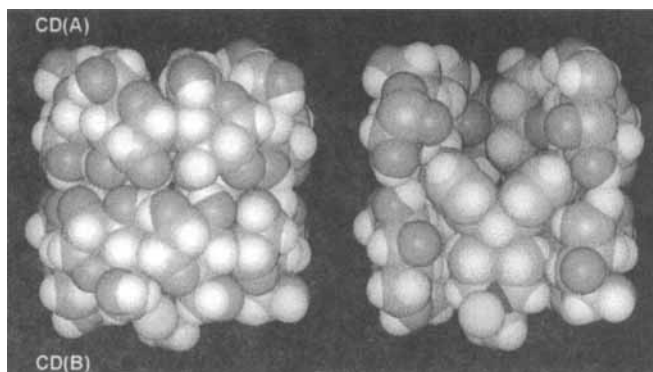


FIGURE 3 Space filling diagrams of the CD(A)-CD(B) dimeric unit showing (left) the extent of guest protrusion and (right) details of guest inclusion revealed by selective deletion of host atoms. (See Color Plate II).

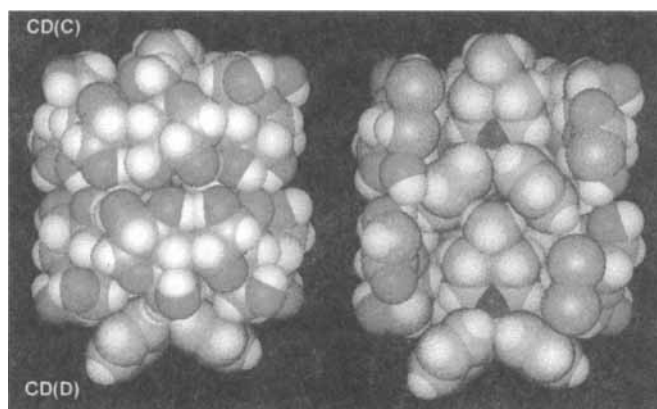


FIGURE 4 Space filling diagrams of the CD(C)-CD(D) dimeric unit showing (left) the extent of guest protrusion and (right) details of guest inclusion revealed by selective deletion of host atoms. (See Color Plate III).

diphenylmethyl residue protrudes slightly from the secondary face of CD(B) into that of CD(A). Thus, while the dimeric interface is occupied by the guest, the cavity region of CD(A) is largely unoccupied. Extended packing diagrams (see below) show that the primary end of CD(A) is partially penetrated by one phenyl group of CYC(D) of the other dimer. The CD(C)–CD(D) dimer (Fig. 4) includes two cyclizine molecules which are in close head-to-tail contact, with the methyl group of CYC(D) engaging in C–H··· $\pi$  interactions with the phenyl rings of CYC(C). The mode of inclusion of CYC(C) in CD(C) is similar to that of CYC(B) in CD(B), with the diphenylmethyl moiety at the dimer interface. However, the inclusion mode for CYC(D) is unique since the methylpiperazine portion of the guest appears to have entered CD(D) from the host primary side, leaving the diphenylmethyl residue protruding significantly from the cavity. As mentioned above, part of this residue is stabilized by penetration into the primary side of CD(A) of the other dimer. Partial protrusion of the methylpiperazine substituents from the primary rims of

CD(B) and CD(C) exposes the piperazine N atoms N2B, N2C which engage in hydrogen bonding to one water molecule each (light blue spheres, Figs. 3, 4). Relevant distances are N2B···O12W 2.79(2) Å and N2C···O25W 2.88(2) Å.

### Host Conformations

The D-glucopyranose rings of all four  $\beta$ -CD molecules adopt the  ${}^4C_1$  conformation. Principal torsion angles defining the macrocyclic conformations are shown in Figure 5 and listed in Table I (average e.s.d. 1°). There is a remarkable consistency in these conformational parameters despite the different modes and extents of inclusion of the guests in the four  $\beta$ -CD molecules. The characteristic shape of the host molecules is confirmed by comparison of the conformational data with the mean values for  $\beta$ -CD molecules [13,14], namely  $|\omega|$  64°,  $\Phi$  112°,  $\psi$  128°,  $\Theta_1$  56°,  $\Theta_2$  –56°. Hydrogen bonds which stabilize the individual  $\beta$ -CD ring conformations and contribute to their ‘roundness’ are those between the O2 and O3

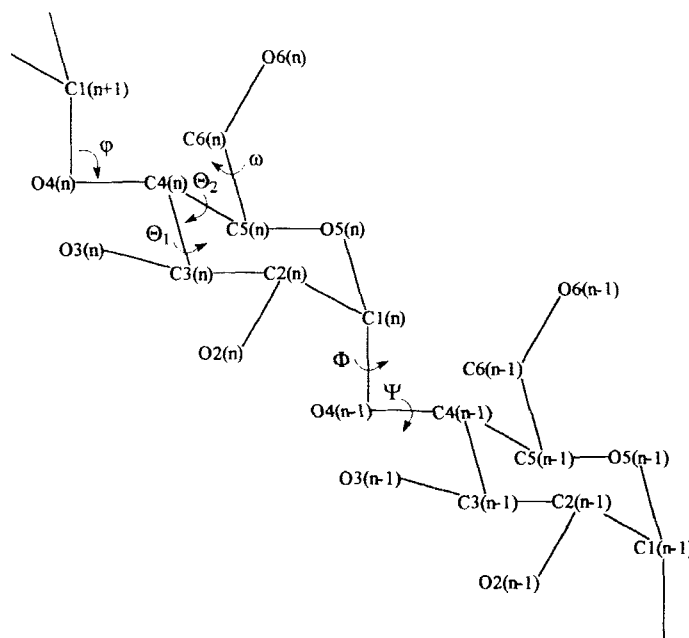


FIGURE 5 Principal torsion angles describing the  $\beta$ -CD conformation.

TABLE I Selected torsion angles for glucose units of the CYCBCD structure

Glucose unit	$\omega(^{\circ})$	$\Phi(^{\circ})$	$\Psi(^{\circ})$	$\Theta_1(^{\circ})$	$\Theta_2(^{\circ})$
A1	-60	110	125	56	-53
A2	-66	116	126	55	-48
A3	+65	116	132	52	-49
A4	-66	116	124	53	-50
A5	-69	113	132	63	-59
A6	-70	112	126	53	-50
A7	-65	111	132	56	-55
A mean	66	113	128	55	-52
B1	-67	115	126	58	-53
B2	-65	116	133	56	-55
B3	-66	109	125	54	-54
B4	-65	111	126	51	-49
B5	-61	115	125	52	-50
B6	-64	116	121	56	-53
B7	+65	115	128	56	-53
B mean	65	114	126	55	-52
C1	-61	116	127	53	-51
C2	-69	114	130	57	-57
C3	-66	114	128	52	-47
C4	-69	113	131	59	-60
C5	-66	111	124	53	-54
C6	-68	112	128	55	-54
C7	-69	116	118	54	-53
C mean	67	114	127	55	-54
D1	-68	111	123	54	-48
D2	-66	116	135	59	-60
D3	-65	111	124	54	-53
D4	-68	111	130	54	-53
D5	-64	110	122	56	-54
D6	-66	117	126	56	-55
D7	-65	116	131	54	-54
D mean	66	113	127	55	-54

hydroxyl groups of neighbouring glucose rings. In this complex, all relevant O2...O3 distances are in the range 2.70(1)–2.88(1) Å. Stabilization of the dimers is achieved by intermolecular O–H...O hydrogen bonding which involves the O3 hydroxyl groups primarily. For dimer CD(A)–CD(B) the O3...O3 distance range is 2.74(1)–3.04(1) Å, while for dimer CD(C)–CD(D), the range is 2.78(1)–3.15(1) Å.

### Guest Conformations

Figure 6 shows the torsion angles  $\delta_1$ ,  $\delta_2$  which define the conformation of the cyclizine molecule. In cyclizine hydrochloride [15,16] these torsion angles are equal and opposite in

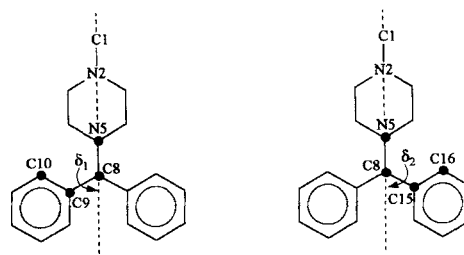


FIGURE 6 Definition of the torsion angles describing the cyclizine conformation.

TABLE II Torsion angles,  $\delta_1$  and  $\delta_2$  for CYC(B), CYC(C) and CYC(D) (e.s.d.'s 1–2 $^{\circ}$ )

Cyclizine	$\delta_1$	$\delta_2$
CYC(B)	-41	44
CYC(C)	-43	44
CYC(D)	-31	53

sign ( $-43.5, 43.5^{\circ}$ ) since the cation is located on a crystallographic mirror plane passing through atoms C1, N2, N5 and C8 (Fig. 1). The values observed for the three independent cyclizine molecules in the complex are listed in Table II, from which it is evident that molecules CYC(B) and CYC(C) adopt symmetrical conformations similar to that found in cyclizine hydrochloride. This is consistent with the 'tight' confinement of these guests at the respective dimer interfaces. However, in CYC(D), the phenyl rings display unsymmetrical twists, this conformation reflecting more guest freedom and being associated with partial inclusion of one only one phenyl ring in CD(A).

### Crystal Structure

Figure 7 is a stereoview showing how the two crystallographically independent  $\beta$ -CD dimeric units associate in the crystal to form a tetramer which is repeated by the screw diad parallel to the  $b$ -axis. Also evident is the extent of inclusion of the guest phenyl groups of CYC(D) and CYC(B) into the primary and secondary faces respectively of CD(A), whose cavity region is empty. Extended packing diagrams are shown in Figure 8 where it is apparent that the

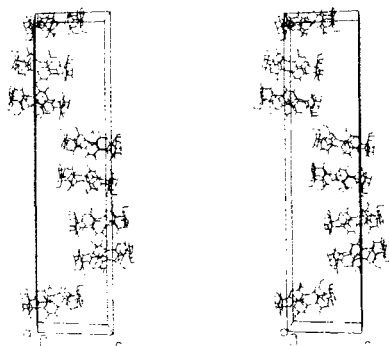


FIGURE 7 Stereoview showing the tetrameric unit in the title complex. (See Color Plate IV).

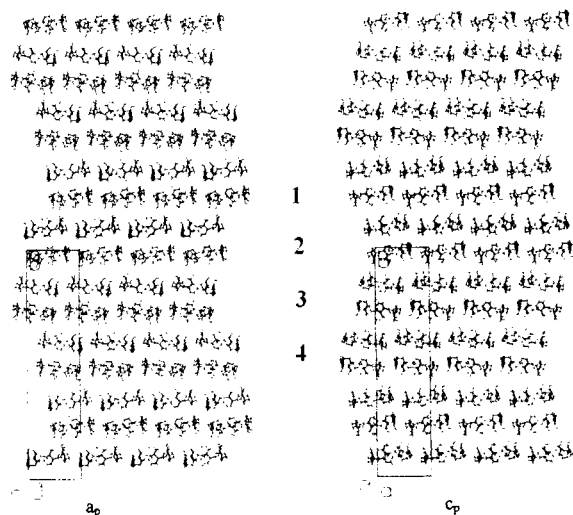


FIGURE 8 Extended packing arrays of the title complex viewed along [001] and [100]. (See Color Plate V).

repeating array in the crystal structure comprises four dimeric layers (1–4). The mean macrocyclic planes of the dimers of layers 1 and 2 are inclined  $10^\circ$  anti-clockwise in their

TABLE III Intralayer interactions for the CYCBCD structure (e.s.d.'s 0.01–0.03 Å)

Type	Layer	Number/dimer	Range(Å)	Mean(Å)
O2...O2	1	2	2.72–2.78	2.75
O6...O6	1	4	2.76–3.01	2.87
O2...O2	2	2	2.76	2.76
O6...O6	2	4	2.80–3.11	2.92
O2...O2	3	2	2.76–2.78	2.75
O6...O6	3	4	2.76–3.01	2.87
O2...O2	4	2	2.76	2.76
O6...O6	4	4	2.80–3.11	2.92

TABLE IV Interlayer interactions for the CYCBCD structure (e.s.d.'s 0.01–0.03 Å)

Type	Layers	Number/dimer	Range(Å)	Mean(Å)
O6...O6	1–2	1	2.97	2.97
O6...O6	2–3	1	2.66	2.66
O6...O6	3–4	1	2.97	2.97
O6...O6	4–1	1	2.66	2.66

respective layer planes, while the  $2_1$ -related layers 3 and 4 tilt  $10^\circ$  clockwise. An important feature of the layer stacking is that in projection down the *b*-axis, all dimeric layers are laterally shifted from one another by more than the radius of a  $\beta$ -CD molecule. These displacements are more readily seen in the *a*- and *c*-axis projections of Figure 8. Crystal cohesion is maintained by intra- and interlayer hydrogen bonds. These are summarized in Tables III and IV. Intralayer hydrogen bonds are primarily of the type O2–H...O2 and O6–H...O6. Interlayer cohesion is effected by a single O6–H...O6 hydrogen bond per dimer unit. The remaining hydrogen bonds in the crystal are those involving water molecules. These are summarized in Table V.

TABLE V Water hydrogen bond interactions for the CYCBCD structure (e.s.d.'s 0.01–0.05 Å)

Type	Number	Number/dimer	Range(Å)	Mean(Å)
O2...Water	20	10	2.73–3.05	2.82
O3...Water	16	8	2.78–3.18	2.92
O6...Water	34	17	2.60–3.15	2.79
Water...Water	43	22	2.70–3.15	2.89

## DISCUSSION

The reported structure has several unique and noteworthy features which confirm our view that novel guest inclusion modes and crystal packing arrangements remain to be discovered for  $\beta$ -CD inclusion complexes. A previous case of a unique packing scheme which we reported was that of the  $\beta$ -CD-diclofenac sodium complex [3], the only  $\beta$ -CD complex known to crystallize in the hexagonal system (space group  $P6_1$ ) and containing a helical array of monomeric complex units. The  $\beta$ -CD-cyclizine complex reported here is remarkably well ordered and serves to illustrate possible structural implications of a 4:3  $\beta$ -CD-guest stoichiometry. Three of the  $\beta$ -CD molecules of the asymmetric unit encapsulate guest molecules in clearly distinguishable modes while the fourth is essentially empty, accommodating guest phenyl residues only at the primary and secondary faces. Such diversity observed in the solid state suggests that similar considerations should be given to interpretation of nmr data in deducing guest inclusion modes in the solution phase.

A search of the Cambridge Crystallographic Database [10] revealed that the  $\beta$ -CD complex with *S*-(-)-*p*-tolylsulfoxide [17,18] has very similar unit cell parameters and crystallizes in the same space group as the title complex. However, the former has 1:1  $\beta$ -CD-guest stoichiometry and its crystal structure is based on tetrameric channel formation with the tetramers packing in the chessboard mode [19]. The extended packing arrays of Figure 8, on the other hand, show that displacements of the dimeric layers in the *xz*-plane eliminate channel continuity beyond that of a single dimeric unit in the present case.

Finally, we attempt to rationalize the formation a 4:3 host-guest unit by drawing on previous findings relating to the inclusion of cyclizine in  $\beta$ -CD and the reported crystal structure. Molecular modelling of the inclusion of the drug in  $\beta$ -CD [12] led to the following conclusions: (a) only the methylpiperazine ring

or one of the phenyl rings of cyclizine can be included within the host molecule; (b) steric hindrance prevents the passage of a cyclizine molecule through the  $\beta$ -CD cavity; (c) inclusion of cyclizine from the secondary side of  $\beta$ -CD is significantly more favorable than inclusion from the primary side. It follows that the observed mode of insertion of cyclizine indicates the direction of its approach during complexation with the  $\beta$ -CD molecule. Furthermore, since we observe from the crystal structure that the preferred inclusion mode is that involving insertion of the methylpiperazine ring in the host cavity, it is reasonable to assume that in solution the preferred species is one in which the methylpiperazine inserts into the larger, secondary hydroxyl side of the host. The tendency for  $\beta$ -CD molecules to form a dimeric head-to-head arrangement in its complexes is also well established [11,19]. With these points in mind, the proposed scheme for complex formation is illustrated in Figure 9. This scheme suggests that two  $\beta$ -CD molecules with cyclizine molecules included from their secondary hydroxyl sides would be unable to form a stable head-to-head dimer due to steric clashes between the diphenylmethyl groups of the included guests. Further, formation of a stable dimer with one included cyclizine molecule could be effected by expulsion of one of the guest molecules, but this would leave one of the  $\beta$ -CD molecules unfilled; insertion of the methylpiperazine ring of a second cyclizine molecule into the primary hydroxyl side would fill this void. The result is a head-to-head  $\beta$ -CD dimer containing two cyclizine molecules in head-to-tail orientation. Crystallization would require efficient packing of such dimers, but the presence of the diphenylmethyl groups protruding from the primary hydroxyl faces would hinder this. The alternatives are (a) expulsion of all cyclizine molecules included from the primary hydroxyl sides and formation of a 4:2 host-guest assembly or (b) as observed here, formation of a 4:3 host-guest assembly in which a compromise is struck

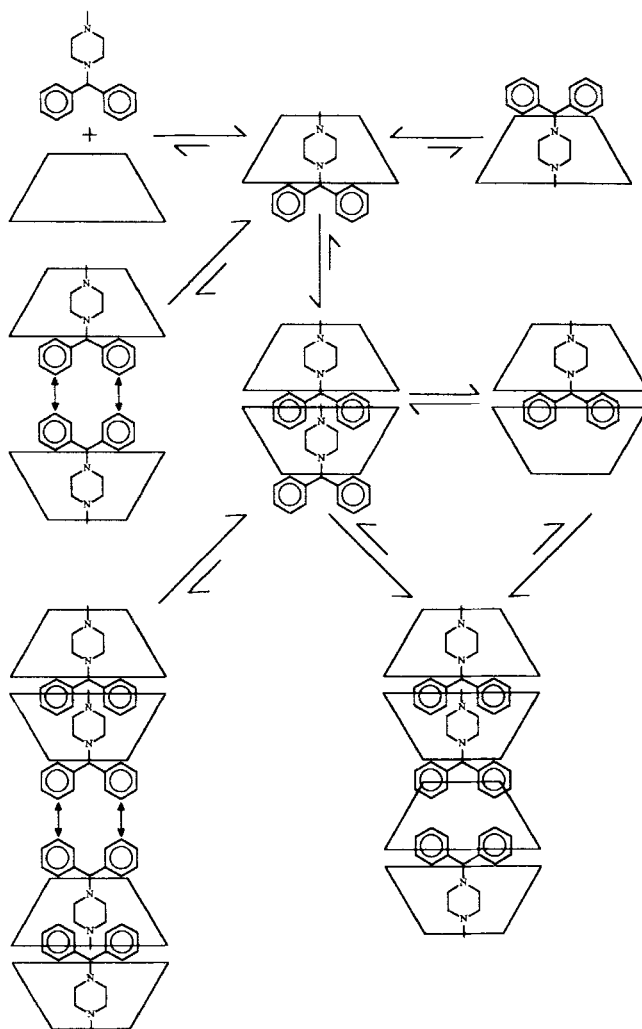


FIGURE 9 Schematic representation of the formation of stable tetrameric units.

between maintaining the guest volume to cavity volume ratio as close to unity as possible and forming a stable crystal with the highest packing efficiency.

## MATERIALS AND METHODS

### Complex Preparation and Preliminary Characterization

$\beta$ -Cyclodextrin was purchased from Cyclolab (Hungary). Cyclizine free base was prepared by dissolving 5 g cyclizine hydrochloride (South

African Druggists International) in distilled water and adding a saturated solution of  $\text{Na}_2\text{CO}_3$  (pH 10.0). The mixture was extracted with ethyl acetate and the latter washed with aqueous saturated NaCl solution, dried over  $\text{MgSO}_4$  and concentrated under reduced pressure to yield the free base (3.7 g, 88% yield). To prepare the inclusion complex, cyclizine (0.30 mmol) was added with vigorous stirring to an aqueous solution of  $\beta$ -CD (0.30 mmol) dissolved in  $4\text{ cm}^3$  distilled water heated to  $60^\circ\text{C}$ . Slow cooling yielded colourless prismatic crystals. For accurate elemental analysis, the crystals were

partially dehydrated under vacuum for 1 h which yielded  $(\beta\text{-CD})_4 \cdot (\text{cyclizine})_3 \cdot 4\text{H}_2\text{O}$  (Calcd. %C 47.38, %H 6.72, %N 1.49, Found. 47.48, 6.66, 1.49). UV spectrophotometry ( $\lambda_{\text{max}} = 225 \text{ nm}$ ) yielded a host-guest ratio of 4:3. Thermogravimetry (TG) and differential scanning calorimetry (DSC) were performed using a Perkin-Elmer PC-7 series thermal analysis system calibrated with indium and zinc standards. TG was carried out on fresh crystals at a scanning rate of  $10^\circ\text{C min}^{-1}$  under a  $\text{N}_2$  gas purge (flow rate  $30 \text{ cm}^3 \text{ min}^{-1}$ ) yielding 14.2% weight loss in the temperature range 30–130°C. This corresponds to 12.5  $\text{H}_2\text{O}$  molecules per CD molecule, confirming the formula of the fully hydrated complex as  $(\beta\text{-CD})_4 \cdot (\text{cyclizine})_3 \cdot 50\text{H}_2\text{O}$ . For DSC, samples in the mass range 5–15 mg were placed in crimped, vented Al pans and heated at  $10^\circ\text{C min}^{-1}$  under a  $\text{N}_2$  gas purge (flow rate  $30 \text{ cm}^3 \text{ min}^{-1}$ ).

### Crystal Structure Analysis

X-ray photography revealed 2/m Laue symmetry and the reflection conditions and intensity statistics indicated the space group  $\text{P2}_1$ . Intensity data were collected on a Nonius Kappa CCD diffractometer from a crystal mounted in mother liquor in a Lindemann capillary. Data were obtained in three sets using  $\phi$  and  $\omega$  scans of  $0.5^\circ$  and 40s ( $2 \times$ ) exposures for each of the 620 frames collected. Data were corrected for Lorentz-polarization effects but not for absorption since this was negligible for the specimen employed. Structure solution was achieved by the Patterson search method using program PATSEE [20] with a head-to-head  $\beta\text{-CD}$  dimer as the search fragment. Partial structure expansion of the correctly placed dimer with SHELX-S [21] yielded most of the atoms of the two remaining  $\beta\text{-CD}$  host molecules. Further refinement with SHELXL-93 [22] and difference

TABLE VI Crystal data and refinement details

Complex formula	$(\text{C}_{42}\text{H}_{70}\text{O}_{35})_4 \cdot (\text{C}_{18}\text{H}_{22}\text{N}_2)_3 \cdot 50(\text{H}_2\text{O})$
Formula weight	6238.92
Temperature	293(1) K
Crystal system	Monoclinic
Space group	$\text{P2}_1$
Unit cell dimensions	$a = 15.246(1) \text{ \AA}$ $b = 65.075(5) \text{ \AA}$ $c = 15.609(1) \text{ \AA}$ $\beta = 102.62(1)^\circ$
Volume	$15112(2) \text{ \AA}^3$
Z	2
Density (calculated)	$1.3713 \text{ g} \cdot \text{cm}^{-3}$
Radiation, wavelength	$\text{MoK}\alpha$ , $0.71069 \text{ \AA}$
Absorption coefficient	$0.1207 \text{ mm}^{-1}$
F (000)	6680.0
Crystal size	$0.4 \times 0.4 \times 0.3 \text{ mm}$
Theta range for data collection	$1.34$ to $26.34^\circ$
Index ranges	$0 \leq h \leq 18$ , $0 \leq k \leq 77$ , $-18 \leq l \leq 18$
Reflections collected	51699
Observed reflections [ $I > 2\sigma(I)$ ]	8806
Independent reflections	22576
Refinement method	blocked-matrix mode on $F^2$
Data/restraints/parameters	22576/1/1747
Goodness-of-fit on $F^2$	0.853
Final R indices [ $I > 2\sigma(I)$ ]	$R_1 = 0.0937$ , $wR^2 = 0.2368$
R indices (all data)	$R_1 = 0.2039$ , $wR^2 = 0.2863$
Largest diff peak and hole	$-0.42, 0.75e \text{ \AA}^{-3}$

electron density maps led to the location of all host and guest atoms and the majority of the water oxygen atoms (41.5 of the 50 calculated from TG data). Water O atoms comprised 31 with s.o.f. 1.0 ( $U_{\text{iso}}$  0.08–0.20 Å<sup>2</sup>) and 14 with s.o.f.'s in the range 0.55–0.95 ( $U_{\text{iso}}$  fixed at 0.20 Å<sup>2</sup>). H atoms were added in idealized positions with separate common variable  $U_{\text{iso}}$  thermal parameters for each  $\beta$ -CD and guest molecule. All atoms were treated isotropically owing to the large number of parameters. Refinement was on  $F^2$  using the blocked-matrix mode with an optimized weighting scheme  $w = [\sigma^2(F_o^2) + (0.167P)^2]^{-1}$  and  $P = [\max(F_o^2, 0) + 2F_c^2]/3$ . Crystal data and further details of the refinement are listed in Table VI.

### Acknowledgements

We thank the University of Cape Town and the NRF (Pretoria) for financial assistance. South African Druggists International kindly provided the cyclizine hydrochloride sample and financial support for this project.

### References

- [1] Szejtli, J. (1998). *Chem. Rev.*, **98**, 1743.
- [2] Schneider, H.-J., Hacket, F. and Rüdiger, V. (1998). *Chem. Rev.*, **98**, 1755.
- [3] Caira, M. R., Griffith, V. J., Nassimbeni, L. R. and van Oudtshoorn, B. (1994). *J. Chem. Soc. Chem. Commun.*, p. 1061.
- [4] Brown, G. R., Caira, M. R., Nassimbeni, L. R. and van Oudtshoorn, B. (1996). *J. Incl. Phenom.*, **26**, 281.
- [5] Caira, M. R., Griffith, V. J., Nassimbeni, L. R. and van Oudtshoorn, B. (1995). *J. Incl. Phenom.*, **20**, 277.
- [6] Caira, M. R., Bourne, S. A. and Mvula, E. (1999). *J. Thermal Anal. Cal.*, **56**, 1329.
- [7] Caira, M. R. and Dodds, D. R. (1999). *J. Incl. Phenom. Macrocyclic Chem.*, **34**, 19.
- [8] Caira, M. R. and Dodds, D. R. (2000). *J. Incl. Phenom. Macrocyclic Chem.*, **38**, 75.
- [9] Penkler, L. J. and Dodds, D. R., *South African Patent Application, ZA99/2097*, 16 March, 1999.
- [10] *Cambridge Structural Database and Cambridge Structural Database System, Version 5.12*, October, 1998, Cambridge Crystallographic Data Centre, University Chemical Laboratory, Cambridge, England.
- [11] Harata, K. (1999). *Chem. Rev.*, **98**, 1803.
- [12] Tong, Q., Lach, J. L., Fong, C. T. and Guillory, J. K. (1991). *Pharm. Res.*, **8**, 1307.
- [13] Lipkowitz, K. B., Green, K. and Yang, J. (1992). *Chirality*, **4**, 205.
- [14] Lichtenthaler, F. W. and Immel, S. (1996). *Liebigs Ann.*, p. 27.
- [15] Gilli, G., Bertolasi, V. and Borea, P. A. (1979). *Eur. Cryst. Meeting*, **5**, 183.
- [16] Bertolasi, V., Borea, P. A., Gilli, G. and Sacerdoti, M. (1980). *Acta Crystallogr.*, **B36**, 1975.
- [17] Fujiwara, T., Tomita, K.-I., Marseigne, I. and Vicens, J. (1988). *Mol. Cryst. Liq. Cryst.*, **156**, 393.
- [18] Vicens, J., Fujiwara, T. and Tomita, K.-I. (1988). *J. Incl. Phenom.*, **6**, 577.
- [19] Mentzafos, D., Mavridis, I. M., le Bas, G. and Tsoucaris, H. (1991). *Acta Crystallogr.*, **B47**, 746.
- [20] Egert, E. and Sheldrick, G. M. (1985). *Acta Crystallogr.*, **A41**, 262.
- [21] Sheldrick, G. M., In: *Crystallographic Computing*, Eds. Sheldrick, G. M., Kruger, C. and Goddard, R., Oxford University Press, **3**, 175.
- [22] Sheldrick, G. M. (1993). *SHELXL-93, Program for Crystal Structure Refinement*, Universität Göttingen, Germany.